

A Continuum Neuronal Model for the Instigation and Propagation of Cortical Spreading Depression

Wei Yao* Huaxiong Huang[†] Robert M. Miura[‡]

December 27, 2010

Abstract

Cortical spreading depression (CSD) waves can occur in the cortices of various brain structures and are associated with the spread of depression of the electroencephalogram signal. In this paper, we present a continuum neuronal model for the instigation and spreading of CSD. Our model assumes that the brain-cell microenvironment can be treated as a porous medium consisting of extra- and intracellular compartments. The main mechanisms in our model for the transport of ions into and out of neurons are cross-membrane ionic currents and (active) pumps, coupled with diffusion in the extracellular space. To demonstrate the applicability of our model, we have carried out extensive numerical simulations under different initial conditions and inclusion of various mechanisms. Our results show that CSD waves can be instigated by injecting cross-membrane ionic currents or by applying KCl in the extracellular space. Furthermore, the estimated speeds of CSD waves are within the experimentally observed range. Effects of specific ion channels, background ion concentrations, extracellular volume fractions, and cell swelling on the propagation speed of CSD are also investigated.

1 Introduction

Cortical spreading depression (CSD) waves in the brain are associated with the spread of depression of the electroencephalogram (EEG) signal. Discovered in 1944 by A.A.P. Leão [13], these waves are characterized by their slow speeds (1-10 mm/min) and their appearance in the cortices of a variety of brain structures in many different animals [1]. While there are many interesting phenomenological aspects of CSD waves, their connection with migraine with aura in humans makes it a particularly important neurophysiological phenomenon from the clinical point of view [6].

Mathematical models of CSD have been proposed almost since the time that CSD was discovered. The cellular automata method developed by Wiener and Rosenblueth [21] for the study of cardiac waves was used by Shibata and Bureš [17] to study CSD. It was postulated early on by Grafstein [4] that potassium was the major ion involved in CSD and that repeated neuronal firings were responsible for the large increase in extracellular potassium. A. Hodgkin proposed a simple single partial differential equation model, essentially the voltage equation in the FitzHugh-Nagumo equations [3, 14] for action potentials, to describe the leading edge of the CSD wave, see Grafstein [5]. Both the cellular automata methods and the simple single PDE model do not lend themselves easily to the incorporation of physiological mechanisms to explain the instigation and propagation of CSD waves. However, the flexibility in using mathematical models based on known and putative physiological mechanisms allows us to perform extensive studies of CSD occurrence, which would be difficult or impossible to perform in the laboratory.

*Department of Mechanics and Engineering Science, Fudan University, Shanghai, China. weiyao6@sohu.com

[†]Department of Mathematics and Statistics, York University, Toronto, Ontario, Canada M3J 1P3. hhuang@yorku.ca

[‡]Department of Mathematical Sciences and Center for Applied Mathematics and Statistics, New Jersey Institute of Technology, Newark, NJ 07102 USA. miura@njit.edu

Kager et al. [9, 10] investigated the instigation of CSD in a single neuron model by using NEURON, a modeling and computational simulation software [7]. By focusing on sodium, potassium, and chloride, three of the main ions in the brain, and ten different ion channels, their simulations produced CSD-like membrane potential depolarizations when stimulated by cross-membrane currents that lasted hundreds of milliseconds. Their NEURON model consisted of representing the neuron by many compartments that corresponded to the morphological structure of the soma and the spatially complex, apical and basal dendritic branches. In a previous paper, we have proposed a discrete neuronal model for the propagation of CSD [8] that extended a simplified model in [9, 10] to a group of neurons. We were able to show that CSD waves spread from one neuron to the next as a natural consequence of the close proximity of the neurons, without **the need of neurotransmitter or cell swelling** required by some earlier models [20, 16]. In particular, we showed that CSD can be instigated by either applying an electrical current stimulus or by injecting KCl in the extracellular medium. We also showed that the depolarization of membrane potential spreads from one neuron to the other, producing a wave-like motion. The spreading speed is consistent with the range of values observed in experiments. Furthermore, using the discrete model, we were able to show that CSD can be instigated and spread even when the fast sodium channel is blocked and no action potentials occur, consistent with experiments **by Sugaya et al. [19]**.

While our discrete model reveals some interesting phenomena, it becomes computationally inefficient when applied to the large scale phenomena observed in experiments. In this paper, we generalize the model in [8] and propose a continuum model. Since the space scale of a CSD wave is large compared to neuron size, we formulate a one-dimensional continuum model by dividing the space into a connected extracellular space overlapping a spatially disconnected intracellular space. The effect of this assumption is that ion diffusion can occur in the extracellular space, but cannot occur in the intracellular space, i.e., intracellular ions would first have to pass through the neuronal membrane and become an extracellular ion before it could diffuse. The model consists of a coupled system of nonlinear diffusion equations for the membrane potential and extra- and intracellular ionic concentrations and accounts for ion movements across neuronal membranes.

The mathematical structure of our model is similar to that of Tuckwell and Miura [20]. As in [20], we assume that ion diffusion is allowed only in the extracellular space. However, there are several important differences between the **model proposed here** and the one proposed in [20]. First of all, our present model allows for intracellular and extracellular volume changes. Second, a fuller repertoire of membrane ionic currents, namely those included in Kager et al. [9, 10], are included. Finally, we incorporate more realistic ionic pumps, as used by Kager et al. [9, 10] in the model.

The main objective of this paper is to use the continuum model to investigate the spreading of CSD and carry out parametric studies (such as changes in the volume fraction as well as in the background concentrations of the ions) and investigate the effects of specific ion channels on the spreading characteristics.

The paper is organized as follows. In Section 2, we present our first mathematical model where only potassium and sodium are considered, following [8, 9]. Numerical simulations are carried out by using two different methods of instigation, i.e., by applying an electrical current stimulus and by injecting potassium chloride. In Section 3, we generalize the model by including cell swelling. In Section 4, we include chloride ions in the model, **following [10]**, and investigate the consequences of neglecting these ions on the spreading of CSD and cell swelling. Effects on the speed of CSD waves due to various factors, such as membrane channels, membrane conductances, and background ion concentrations are investigated. In Section 5, we provide a brief summary of our results and conclusions and a discussion of future directions.

2 A continuum model without cellular volume change

We now formulate a continuum model for CSD, in the same spirit as the one-dimensional spatial continuum modeling approach used by Tuckwell and Miura (TM) [20], with the ionic currents in the TM model replaced by those in Kager et al. [9]. Following Kager et al. [9], we first consider the case with only two ions, sodium, Na, and potassium, K, with extra- and intracellular concentrations

denoted by $[ion]_e$ and $[ion]_i$ (mM/cm³), respectively, where $ion=Na$ and K . In addition, we consider two compartments that represent the extra- and intracellular spaces. The membrane potential E_m is governed by the differential equation

$$C_m \frac{\partial E_m}{\partial t} = -I \quad (1)$$

where C_m is the membrane capacitance per unit surface area (farad/cm²) and I is the total cross-membrane ionic current per unit surface area (mA/cm²). The total cross-membrane current is given by the sum of the sodium currents, $I_{Na} = I_{Na,T} + I_{Na,P} + I_{Na,Leak} + I_{Na,Pump}$, the potassium currents, $I_K = I_{K,DR} + I_{K,A} + I_{K,Leak} + I_{K,Pump}$, and the leak current, I_{Leak} . An additional stimulus current, I_{Sti} , will be included to trigger CSD when the soma allows action potentials. If the neuron has been treated with tetrodotoxin (TTX), there are no action potentials and the $I_{Na,T}$ current is removed from the model, see [19]. In the latter case, CSD will be triggered by using a different type of stimulus, e.g., application of KCl, which could be easily modeled by changing the initial condition of potassium. The cross-membrane currents are modeled using: 1) the Goldman-Hodgkin-Katz (GHK) formulas for the active membrane currents, namely, the fast transient sodium current, $I_{Na,T}$, the persistent sodium current, $I_{Na,P}$, the potassium delayed rectifier current, $I_{K,DR}$, and the transient potassium current, $I_{K,A}$; 2) the Hodgkin-Huxley (HH) model for the leak currents, namely, the sodium leak current, $I_{Na,Leak}$, the potassium leak current, $I_{K,Leak}$, and the fixed leak current, I_{Leak} ; and 3) the sodium-potassium exchange pump currents, $I_{Na,Pump}$ and $I_{K,Pump}$.

The GHK current is suitable when there is a large difference in concentrations in the ICS and ECS compartment, as argued by Koch and Segev [11]. The general expressions for the GHK and HH types of currents are given by

$$I_{ion,GHK} = g_{ion,GHK} m^p n^q \frac{F E_m \left([ion]_i - \exp\left(-\frac{E_m}{\phi}\right) [ion]_e \right)}{\phi \left(1 - \exp\left(-\frac{E_m}{\phi}\right) \right)}, \quad (2)$$

$$I_{ion,HH} = g_{ion,HH} (E_m - E_{ion}) \quad (3)$$

where $g_{ion,GHK}$ is the product of the conductance amplitude and membrane permeability for the active currents and $g_{ion,HH}$ is the conductance amplitude for the passive currents where $ion=Na$ and K , m and n are the activation and inactivation gating variables, respectively, for the different GHK-modeled channels that are ion-specific [9]. Note that the conductances $g_{ion,HH}$ for the leak currents are assumed to be constant. $\phi = RT/F$ is a parameter where R is the universal gas constant, T the absolute temperature, and F the Faraday constant. Finally, E_{ion} is the Nernst potential for $ion = Na$ and K , given by

$$E_{ion} = \phi \log \frac{[ion]_e}{[ion]_i}. \quad (4)$$

In addition to the ion-specific leak currents, there is a general leak current given by

$$I_{Leak} = g_{HH} (E_m + 70) \quad (5)$$

where g_{HH} is a constant conductance. This current drives the membrane potential towards a rest state of -70 mV. The pump currents are given by $I_{Na,Pump} = 3I_{Pump}$ and $I_{K,Pump} = -2I_{Pump}$. **The equation for the pump is given in [12], but in order to obtain the same equilibrium sodium and potassium concentrations given there, we had to change the pump formula to the following expression**

$$I_{Pump} = \frac{I_{max}}{(1 + 2.0[K]_e^{-1})^2 (1 + 7.7[Na]_i^{-1})^3}. \quad (6)$$

The concentrations of the ions are governed by the following coupled system of nonlinear diffusion equations

$$\frac{\partial[Na]_e}{\partial t} = \frac{S}{FV_i f} I_{Na} + D_{Na} \frac{\partial^2[Na]_e}{\partial x^2}, \quad (7)$$

$$\frac{\partial[Na]_i}{\partial t} = -\frac{S}{FV_i} I_{Na}, \quad (8)$$

$$\frac{\partial[K]_e}{\partial t} = \frac{S}{FV_i f} I_K + D_K \frac{\partial^2[K]_e}{\partial x^2}, \quad (9)$$

$$\frac{\partial[K]_i}{\partial t} = -\frac{S}{FV_i} I_K \quad (10)$$

where S is the cell surface area (in cm^2), V_i , and V_e are the intra- and extracellular volumes (in cm^3), and $f = V_e/V_i$. The effects of osmotic water movements are ignored in this model, and consequently the extra- and intracellular volumes are constant.

The gating variables m and h satisfy the following equations

$$\frac{dm}{dt} = \alpha_m(1 - m) - \beta_m m, \quad (11)$$

$$\frac{dh}{dt} = \alpha_h(1 - h) - \beta_h h, \quad (12)$$

and the values of α and β are given in Table 1, along with the exponents p and q [9]. The extracellular volume is assumed to be 15% of the intracellular value, i.e., $V_e = 0.15V_i$ [9]. Other relevant parameter values are: $R = 8.31$ (mV coulomb/mM K), $F = 96.485$ coulomb/mM. Finally, we note that the ion concentrations are conventionally measured in mM/liter, while in equations (7)-(10), the correct unit is mM/ cm^3 . Thus, a scale factor of 10^{-3} needs to multiply the right-hand sides of equations (7)-(10).

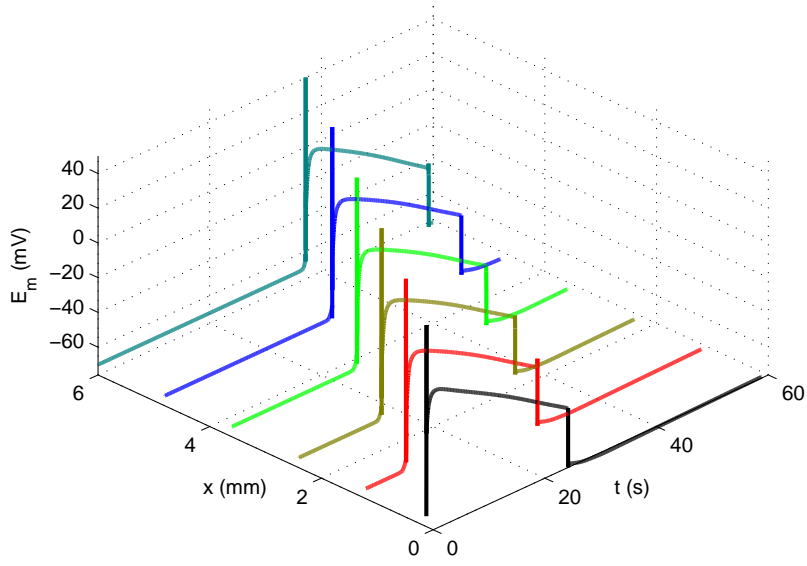
As in [8], the initial resting values are obtained by running the model equations until a steady state is reached. The values are given in Table 2. **In [8], we initiated CSD waves by using electrical stimuli when $I_{Na,T}$ is present or by increasing the concentration of potassium near the origin when $I_{Na,T}$ is present or not present. Throughout this paper, we will use the potassium stimulus that leads to an initial condition on $[K]_e$, which we assume is Gaussian with a peak value of 50 mM/liter, given by**

$$[K]_e(x, 0) = [K]_{e,rest} + [K]_{max} \exp\left(-\frac{x^2}{2\epsilon^2}\right). \quad (13)$$

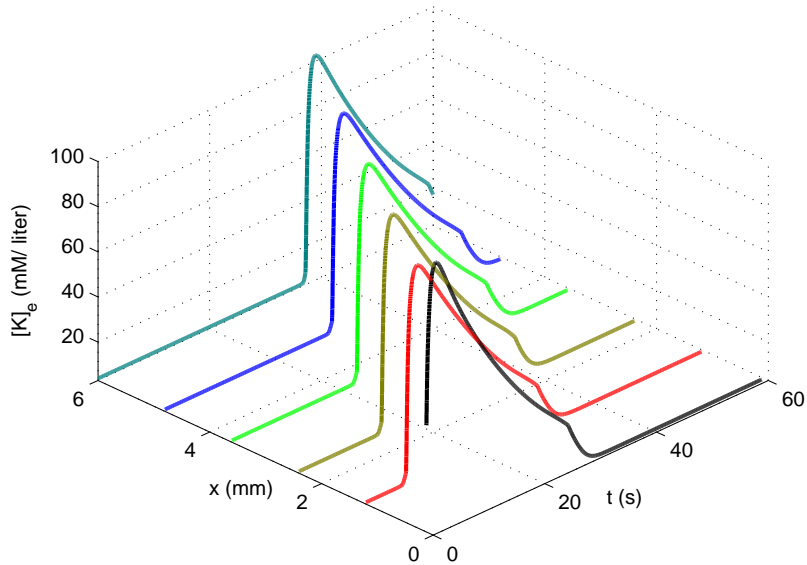
The set of partial differential equations (7)-(10) are solved on a spatial domain $0 < x < L$ where L is chosen to be 6 mm in this paper. The equations are first discretized by replacing the partial derivatives in x by difference formulas on equally distributed grid points $0 = x_1 < x_2 < \dots < x_N = L$ with size δx . This leads to a system of nonlinear stiff ordinary differential equations for $[Na]_e$, $[Na]_i$, $[K]_e$, $[K]_i$, and E_m on the grid points x_j , $j = 1, \dots, L$, which are solved using a built-in Matlab solver `ode15s`, with proper initial and boundary conditions. In Fig. 1, we have plotted the time histories of the membrane potential and the extracellular potassium concentration where **an initial KCl stimulus is applied near $x = 0$ mm**. We have used $\epsilon = 0.5 \times 10^{-2}$ mm. It can be seen clearly that the depolarization of membrane potential follows the increase of extracellular potassium concentration in both cases.

2.1 Effects of $I_{Na,T}$

To investigate the effects of the fast transient Na current on CSD propagation, we considered two different paradigms: 1) with action potentials and 2) without action potentials. For the first case, the fast transient sodium current, $I_{Na,T}$ is included in the equations to produce action potentials, and CSD is instigated by using a **potassium** stimulus, as noted above. In the second case, we



(a)



(b)

Figure 1: Time histories of (a) membrane potential and (b) extracellular concentration of potassium at different spatial locations when I_{NaT} currents are present. **Note that there is an action potential at the leading edge of the membrane potential wave as it first passes threshold for the generation of a spike. The initial Gaussian potassium stimulus is centered at $x = 0$ mm with $\epsilon = 0.5 \times 10^{-2}$ mm.**

Table 1: Parameter values for active membrane ionic currents.

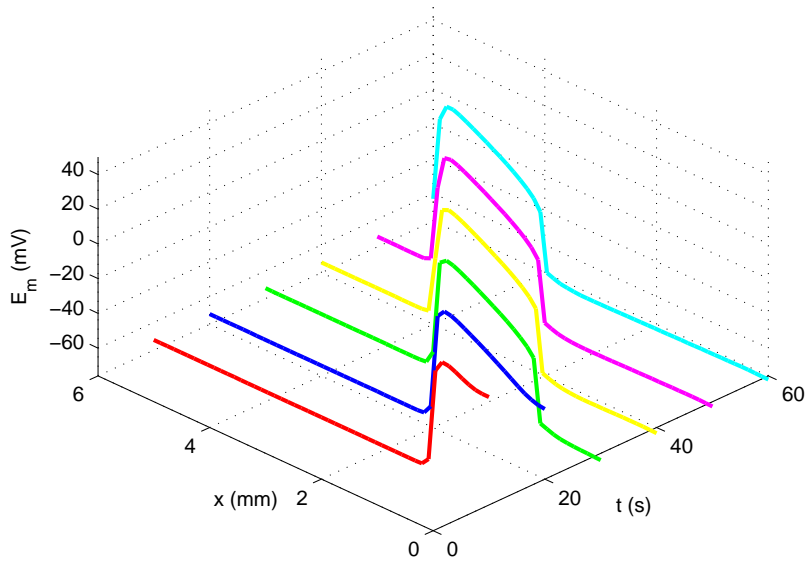
Currents mA/cm ²	$g_{ion,GHK}$ S/cm ²	Gates $m^p h^q$	Voltage-Dependent Rate Constants
$I_{Na,T}$	100×10^{-5}	$m^3 h$	$\alpha_m = 0.32 \frac{E_m + 51.9}{1 - \exp[-(0.25E_m + 12.975)]}$ $\beta_m = 0.28 \frac{E_m + 24.89}{\exp[0.2E_m + 4.978] - 1}$ $\alpha_h = 0.128 \exp[-(0.056E_m + 2.94)]$ $\beta_h = \frac{4}{1 + \exp[-(0.2E_m + 6)]}$
$I_{Na,P}$	2×10^{-5}	$m^2 h$	$\alpha_m = \frac{1}{6(1 + \exp[-(0.143E_m + 5.67)])}$ $\beta_m = \frac{\exp[-(0.143E_m + 5.67)]}{6(1 + \exp[-(0.143E_m + 5.67)])}$ $\alpha_h = 5.12 \times 10^{-8} \exp[-(0.056E_m + 2.94)]$ $\beta_h = \frac{1.6 \times 10^{-6}}{1 + \exp[-(0.2E_m + 8)]}$
$I_{K,DR}$	100×10^{-5}	m^2	$\alpha_m = 0.016 \frac{E_m + 34.9}{1 - \exp[-(0.2E_m + 6.98)]}$ $\beta_m = 0.25 \exp[-(0.25E_m + 1.25)]$
$I_{K,A}$	10×10^{-5}	$m^2 h$	$\alpha_m = 0.02 \frac{E_m + 56.9}{1 - \exp[-(0.1E_m + 5.69)]}$ $\beta_m = 0.0175 \frac{E_m + 29.9}{\exp(0.1E_m + 2.99) - 1}$ $\alpha_h = 0.016 \exp[-(0.056E_m + 4.61)]$ $\beta_h = \frac{0.5}{1 + \exp[-(0.2E_m + 11.98)]}$
I_{NMDA}	10×10^{-5}	mh	$\alpha_m = \frac{0.5}{1 + \exp\left[\left(\frac{13.5 - [K]_e}{1.42}\right)\right]}$ $\beta_m = 0.5 - \alpha_m$ $\alpha_h = \frac{1}{2000 \left(1 + \exp\left[\frac{[K]_e - 6.75}{0.71}\right]\right)}$ $\beta_h = 0.0005 - \alpha_h$

set the fast transient sodium current to zero, i.e., effectively treating the cortex with tetrodotoxin (TTX). In Fig. 2, we have plotted the spatial and temporal variations of the membrane potential and the extracellular potassium concentration with the fast sodium channels blocked. It is clear that blocking the fast sodium channels does not prevent the instigation and spreading of CSD.

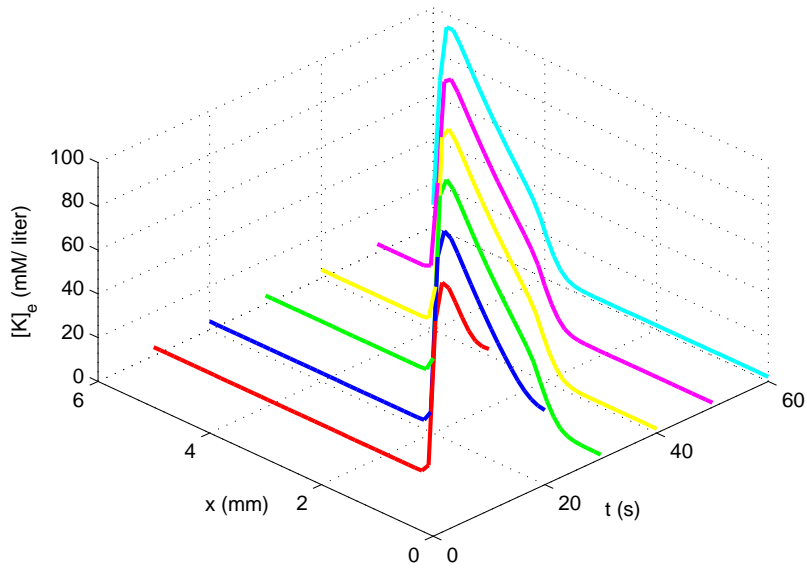
To provide a clearer view of the CSD wave, we have plotted the propagation of membrane depolarization triggered by the injection of $[K]_e$ in Fig. 3, with and without the fast sodium channel. Plotted in Fig. 4 are the corresponding propagations of $[K]_e$. It can be seen that the spreading speed is much slower without the fast sodium channel current.

2.2 Effects of volume fraction, f , and background ion concentrations

The volume fraction, $f = V_e/V_i$, i.e., the ratio of the extracellular space volume, V_e , to the intracellular space volume, V_i , could vary in the brain-cell microenvironment. The background ion concentrations could also fluctuate. To examine the effects of volume fraction and background ion concentration, we studied the cases: $f = 0.15, 0.25$, and 1, corresponding to increasing extracellular volume relative to the intracellular volume. In addition, we also change the background ion

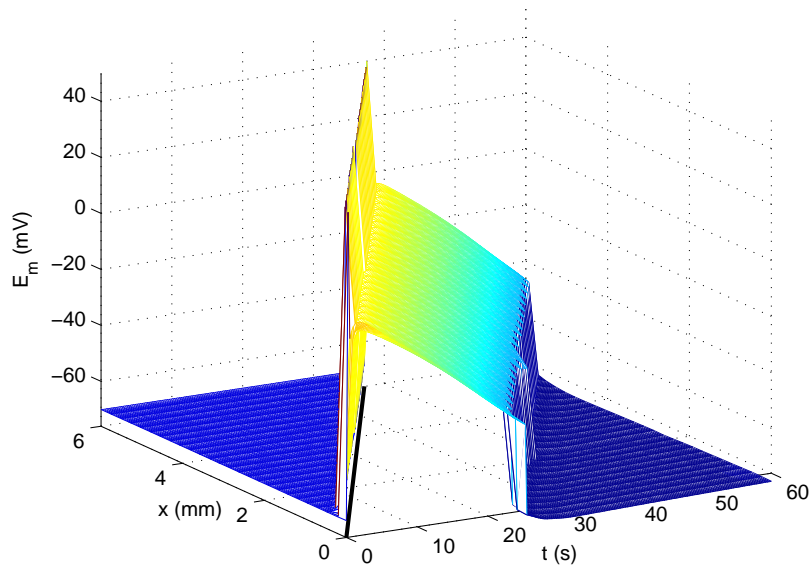


(a)

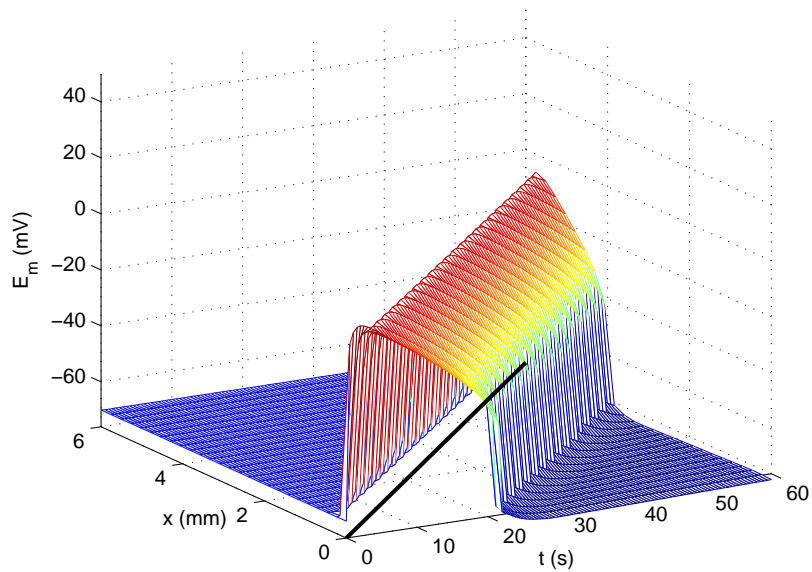


(b)

Figure 2: Traveling wave profiles of (a) membrane potential and (b) extracellular concentration of potassium at different times with the I_{NaT} channels blocked **and initial potassium stimulus near $x = 0$** .

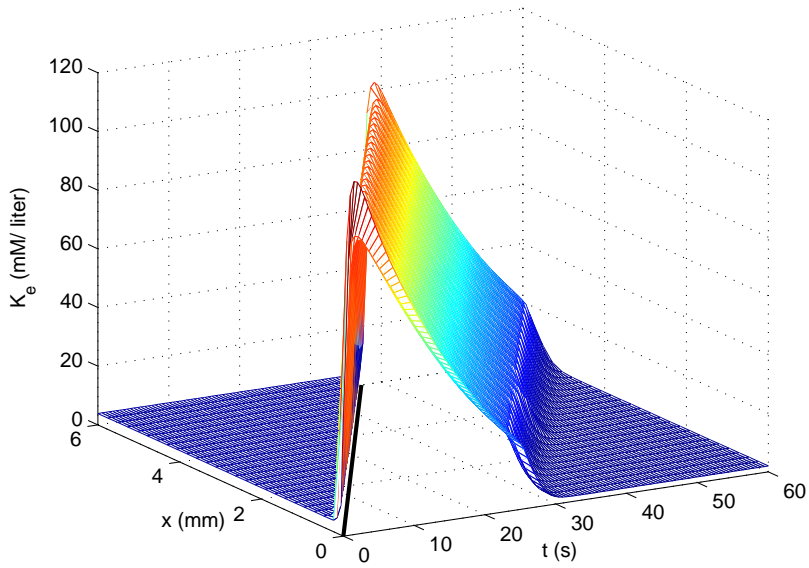


(a)

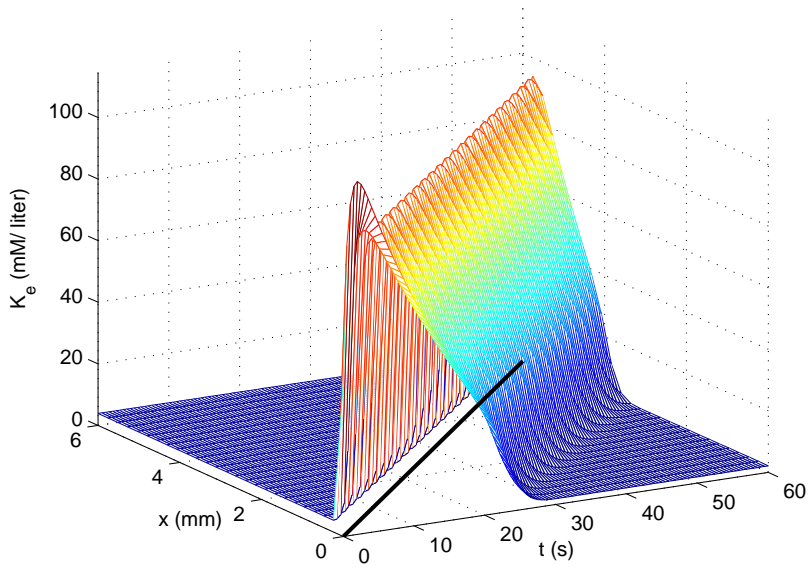


(b)

Figure 3: Propagation of the depolarization of membrane potential for $f = 0.15$: (a) with the fast transient sodium channel, and (b) without the fast transient sodium channel. **The speed of the CSD depolarization wavefront is determined by the slope of the black line in the (x, t) -plane in each figure. The CSD waves are instigated by a potassium stimulus.**



(a)



(b)

Figure 4: Propagation of $[K]_e$ for $f = 0.15$: (a) with the fast transient sodium channel, and (b) without the fast transient sodium channel. **The speed of the CSD depolarization wavefront is determined by the slope of the black line in the (x, t) -plane in each figure. The CSD waves are instigated by a potassium stimulus.**

Table 2: Initial resting values for the computations. **The first six parameter values are from [9] and the remaining 11 equilibrium parameter values are close to those given in [9] and are obtained using the revised pump equation (6).**

Parameter	Value	Unit
d_S (diameter of soma)	5.45×10^{-4}	cm
A_S (surface of soma)	1586×10^{-8}	cm ²
V_S (volume of soma)	2160×10^{-12}	cm ³
C_m (membrane capacitance)	7.5×10^{-5}	s / Ω cm ²)
I_{max}	0.013	mA / cm ²
E_m	-70	mV
$[K]_e$	3.86	mM/liter
$[K]_i$	133.45	mM/liter
$[Na]_e$	141.6	mM/liter
$[Na]_i$	9.82	mM/liter
$[Cl]_e$	113.5	mM/liter
$m_{Na,T,0}$ (initial value of m for $I_{Na,T}$)	5×10^{-3}	
h_{T0} (initial value of h for $I_{Na,T}$)	0.995	
m_{P0} (initial value of m for $I_{Na,P}$)	1.3×10^{-2}	
m_{KDR0} (initial value of m for $I_{K,DR}$)	1.3×10^{-3}	
m_{KA0} (initial value of m for $I_{K,A}$)	0.12	
h_{KA0} (initial value of h for $I_{K,A}$)	0.12	

concentrations to $[K]_e = 4.43$, $[K]_i = 133.4$, $[Na]_e = 109.0$, and $[Na]_i = 14.7$, which are equilibrium values obtained by using the pump in [9], instead of the values given in Table 2, which are used for previous computations. The case of $f = 1$ corresponds to equal extra- and intracellular volumes, which is unrealistic physiologically, but serves as a simple control case for comparison. Our numerical computations show that the speed, v_f , of a CSD wave, relative to its speed for $f = 1$, v_1 , decreases as f increases, consistent with an expanded extracellular space leading to a slower temporal buildup of extracellular potassium concentration. The estimated speeds are given in Table 3.

Table 3: Speeds of the CSD waves for different volume fractions, $f = V_e/V_i$, with and without the fast transient sodium current, $I_{Na,T}$.

Background Ion Concentrations	$f = V_e/V_i$ Volume Fraction	0.15	0.25	1.0
	$\sqrt{1/f}$	2.58	2.0	1.0
Equilibrium Values (Table 2)	$I_{Na,T}$ active	9.68	8.14	4.02
	v_f/v_1 ($I_{Na,T}$ active)	2.41	2.02	1
	$I_{Na,T}$ inactive	6.08	3.72	2.06
	v_f/v_1 ($I_{Na,T}$ inactive)	2.25	1.81	1
New Equilibrium Values	$I_{Na,T}$ active	5.60	5.10	3.00
	v_f/v_1 ($I_{Na,T}$ active)	1.87	1.70	1
	$I_{Na,T}$ inactive	3.00	2.80	1.80
	v_f/v_1 ($I_{Na,T}$ inactive)	1.67	1.56	1

3 A continuum model with cell swelling

If **changes in the volume** due to osmosis are incorporated into our model, then the equations are given by

$$\frac{\partial(\hat{f}[Na]_e)}{\partial t} = \frac{S}{FV}I_{Na} + \frac{\partial}{\partial x} \left(\hat{f}D_{Na} \frac{\partial[Na]_e}{\partial x} \right), \quad (14)$$

$$\frac{\partial((1-\hat{f})[Na]_i)}{\partial t} = -\frac{S}{FV}I_{Na}, \quad (15)$$

$$\frac{\partial(\hat{f}[K]_e)}{\partial t} = \frac{S}{FV}I_K + \frac{\partial}{\partial x} \left(\hat{f}D_K \frac{\partial[K]_e}{\partial x} \right), \quad (16)$$

$$\frac{\partial((1-\hat{f})[K]_i)}{\partial t} = -\frac{S}{FV}I_K, \quad (17)$$

where $\hat{f} = V_e/V$ and $V = V_e + V_i$ is the total volume (cytoplasmic plus interstitial). Note that \hat{f} and $f = V_e/V_i$ are related by the expression $1/\hat{f} = 1 + 1/f$.

Rearranging the equations, we obtain

$$\frac{\partial[Na]_e}{\partial t} = \frac{S}{FV\hat{f}}I_{Na} - \frac{[Na]_e}{\hat{f}} \frac{\partial\hat{f}}{\partial t} + \frac{D_{Na}}{\hat{f}} \frac{\partial}{\partial x} \left(\hat{f} \frac{\partial[Na]_e}{\partial x} \right), \quad (18)$$

$$\frac{\partial[Na]_i}{\partial t} = -\frac{S}{FV(1-\hat{f})}I_{Na} + \frac{[Na]_i}{1-\hat{f}} \frac{\partial\hat{f}}{\partial t}, \quad (19)$$

$$\frac{\partial[K]_e}{\partial t} = \frac{S}{FV\hat{f}}I_K - \frac{[K]_e}{\hat{f}} \frac{\partial\hat{f}}{\partial t} + \frac{D_K}{\hat{f}} \frac{\partial}{\partial x} \left(\hat{f} \frac{\partial[K]_e}{\partial x} \right), \quad (20)$$

$$\frac{\partial[K]_i}{\partial t} = -\frac{S}{FV(1-\hat{f})}I_K + \frac{[K]_i}{1-\hat{f}} \frac{\partial\hat{f}}{\partial t}. \quad (21)$$

According to Shapiro [15] (page 225), the rate of water flow due to an osmotic pressure difference can be written as

$$\frac{\partial\hat{f}}{\partial t} = -\frac{P_f V_w S}{V} ([ion]_i - [ion]_e) \quad (22)$$

where P_f ($=3 \times 10^{-3}$ cm/ms) is the osmotic water permeability of the membrane and V_w ($=1.8 \times 10^{-5}$ litre/mM) is the partial molar volume of water. Since we only consider sodium and potassium in this section, we modify this relationship by assuming that the imbalance is offset by immobile ions that cannot cross the membrane. The new equation is given by

$$\frac{\partial\hat{f}}{\partial t} = -\frac{P_f V_w S}{V} \left([Na]_i + [K]_i - [Na]_e - [K]_e + \frac{V_{i_0}}{V_i} A \right) \quad (23)$$

where $A = [Na]_{e,0} + [K]_{e,0} - [Na]_{i,0} - [K]_{i,0}$. When $\partial\hat{f}/\partial t$ is negative, during cell swelling, the total intracellular concentration of the ions decreases, while the total extracellular concentration increases. **In this paper, we have also imposed a constraint that the volume fraction stays within a range between minimum (5%) and maximum (95%) values.**

Fig. 5 shows that the cell volume fraction ($=V_i/V$) increases during the spreading of CSD propagation, **see Somjen [18] and references therein.** We can see that at $x = 0$, the location where the initial **potassium** stimulus is applied, the cell shrinks first due to the initial increase of $[K]_e$. The cell eventually swells after the depolarization of membrane and the influx of ions. Fig. 6 **shows the time histories of the membrane potential and the extracellular potassium concentration during potassium-stimulated CSD wave propagation.** Compared to the results obtained earlier when volume change is not allowed, the wave speed is nearly the same, but it takes longer for the neurons to repolarize when they are allowed to swell.

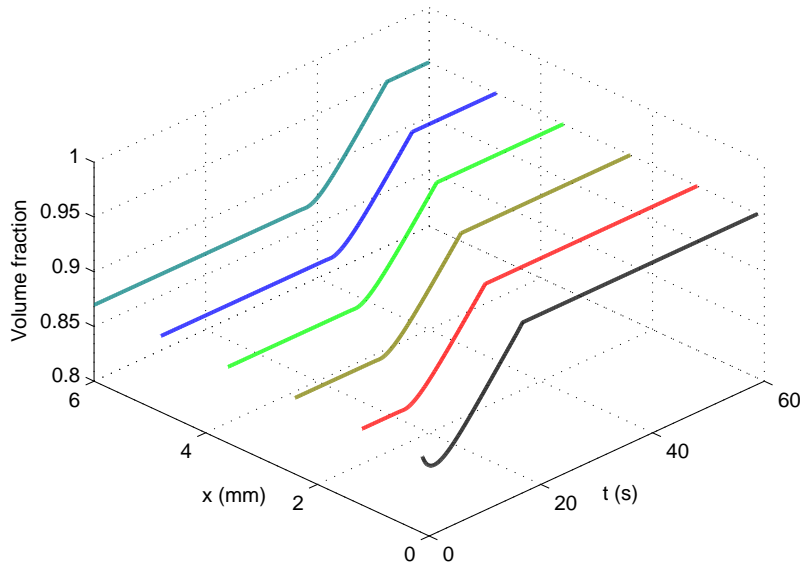


Figure 5: Volume fraction as a function of time at selected spatial locations during CSD propagation.

4 A continuum model including chloride and cell swelling

We now extend our model by including the chloride anion, Cl . This can be done by replacing the general leak current term $I_{Leak} = g_{HH}(E_m + 70)$ with the Cl leak current

$$I_{Cl^-,HH} = g_{HH} \left(E_m + \phi \log \frac{[Cl]_e}{[Cl]_i} \right), \quad (24)$$

and add the following equations

$$\frac{\partial [Cl]_e}{\partial t} = \frac{S}{FV\hat{f}} I_{Cl} - \frac{[Cl]_e}{\hat{f}} \frac{\partial \hat{f}}{\partial t} + \frac{D_{Cl}}{\hat{f}} \frac{\partial}{\partial x} \left(\hat{f} \frac{\partial [Cl]_e}{\partial x} \right), \quad (25)$$

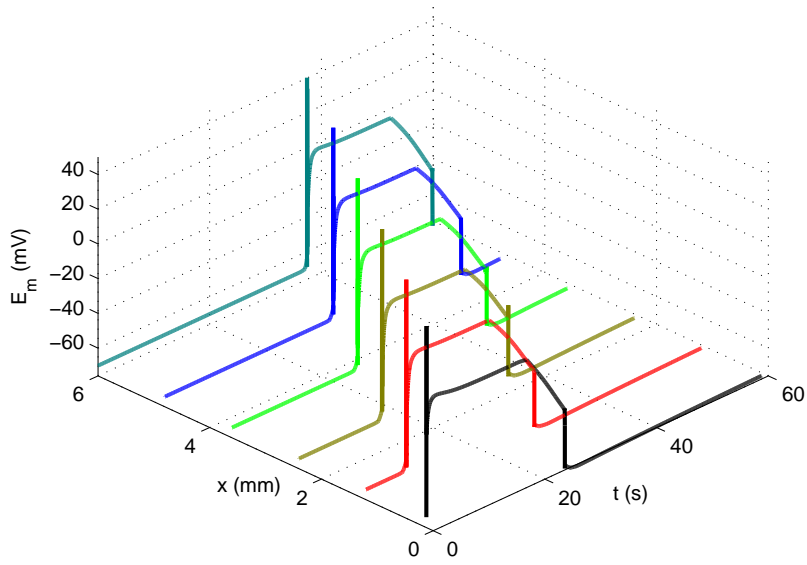
$$\frac{\partial [Cl]_i}{\partial t} = -\frac{S}{FV(1-\hat{f})} I_{Cl} + \frac{[Cl]_i}{1-\hat{f}} \frac{\partial \hat{f}}{\partial t}. \quad (26)$$

As Cl is the only extracellular anion in our simulations, its initial extracellular concentration, $[Cl]_{e,o}$, was determined by the sum of both cations: $[Cl]_{e,o} = [Na]_{e,o} + [K]_{e,o}$, to ensure electroneutrality. We chose the intracellular concentration of chloride, $[Cl]_i$, so that isotonicity is achieved. Table 4 lists the estimated CSD propagation speeds under different conditions. We can see that including Cl affects the speed of CSD while the effect of cell swelling is negligible.

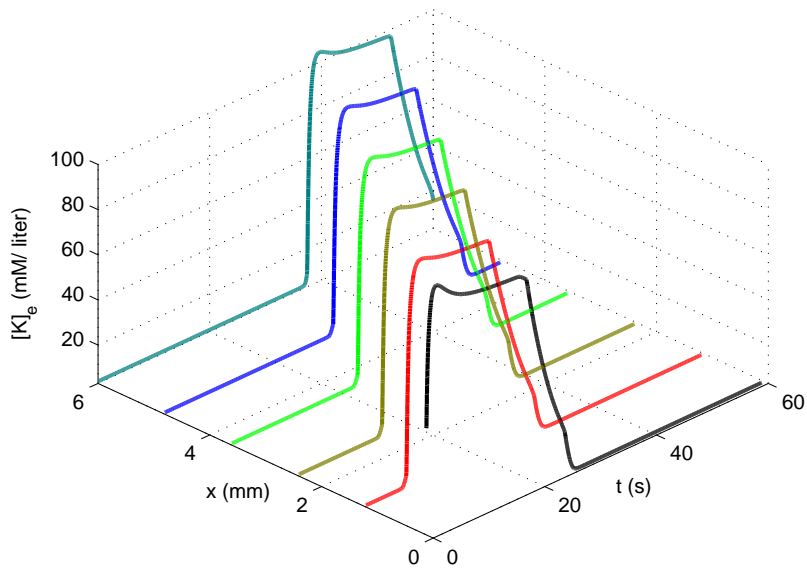
Fig. 7 shows that the $[Cl]_e$ change is less when cells are allowed to swell. This is due to the fact that when cells swell, the ECS space is reduced, which increases the extracellular concentrations. Fig. 7 also shows that when the cell volume reaches its maximum value (0.95 V), this effect is less profound.

5 Conclusions

The main objective of this paper is to investigate whether the spreading of CSD is a natural physical process of the brain-cell microenvironment after its initiation, and we have focused on neurons and

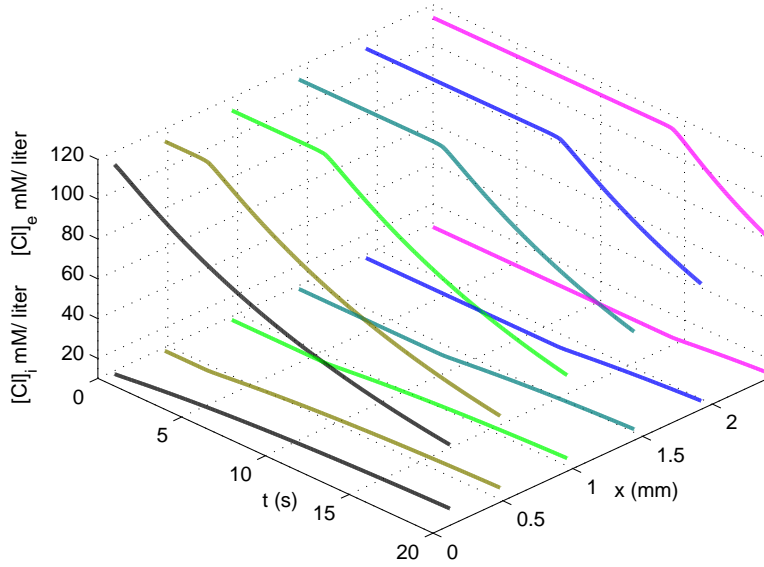


(a)

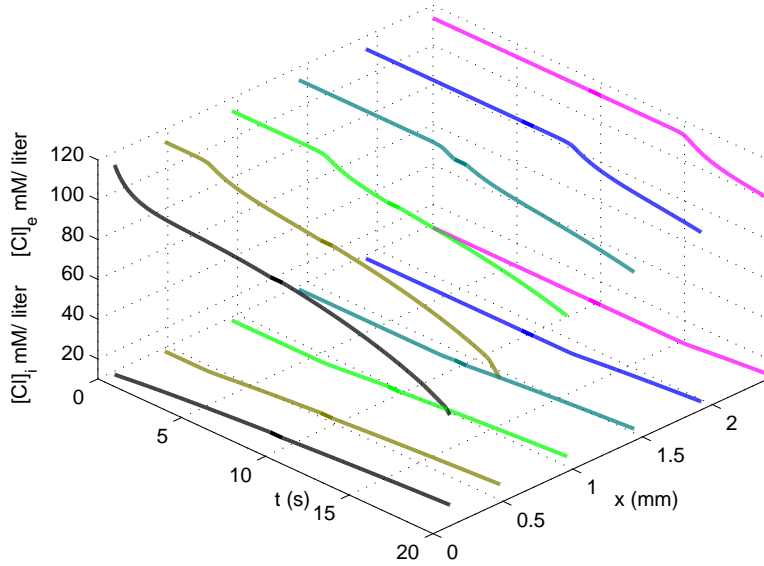


(b)

Figure 6: Time histories of (a) membrane potential and (b) extracellular concentration of potassium during potassium stimulated CSD propagation with cell swelling incorporated into the model.



(a)



(b)

Figure 7: Extracellular and intracellular Cl concentrations versus time: (a) without and (b) with cell swelling during potassium-instigated CSD wave.

Table 4: CSD propagation speeds affected by model components.

Model Components	Speed (mm/min)
Na and K only	9.68
Na, K, and Cl	10.12
Na, K, and Cell Swelling	9.61
Na, K, Cl, and Cell Swelling	10.10

the roles played by major ions. We have presented a continuum neuronal model for the instigation and spreading of cortical spreading depression. Our model is based on the assumption that the brain-cell microenvironment can be treated as a porous medium consisting of neuronal and extracellular compartments. The main mechanisms for ion transport employed in our model are cross-membrane (passive and active) currents and (active) pumps, coupled with diffusion in the extracellular space. To demonstrate the applicability of our model, we have carried out extensive numerical simulations under various conditions. Our results show that the spreading of CSD can be instigated by injecting KCl in the extracellular space. Furthermore, the estimated speed of CSD is within the experimentally observed range. Effects of specific ion channels, background ion concentrations, extracellular volume fractions, and cellular swelling on the spreading speed was also investigated.

We are in the process of incorporating the functions of glial cells as well as the roles played by other important substances such as glutamate and ATP. It is well known that CSD is often accompanied by vasodilation and vasoconstriction. Recent experiments also show that the threshold for CSD in female mice is lower than that for male mice [2]. These findings suggest that further theoretical studies of CSD is needed. For example, it would be of both theoretical and practical importance to examine the effects of **CSD on vasodilation/vasoconstriction and neurovascular coupling**. It will also be of interest to find out whether we can identify physiological or anatomical indicators that would explain these important findings, thus helping us to understand the organization and functionality of the brain. These will be the subjects of future investigations.

Acknowledgement

We would like to acknowledge financial support from the Chinese Ministry of Education and MITACS (WY), NSERC and MITACS (HH), and NSF (RMM). Part of the work was done when WY was a visiting researcher at York University.

References

- [1] BUREŠ, J., BUREŠOVÁ, O., AND KŘIVÁNEK, J. 1974. *The Mechanism and Applications of Leão's Spreading Depression of Electroencephalographic Activity*. Academia, Prague.
- [2] BRENNAN, K.C., REYES, M.R., VALDÉS, H.E.L., ARNOLD, A.P., AND CHARLES, A.C. 2007. Reduced threshold for cortical spreading depression in female mice. *Ann. Neurol.* **61**, 603–606.
- [3] FITZHUGH, R. 1961. Impulses and physiological states in theoretical models of nerve membrane. *Biophys. J.* **1** 445–466.
- [4] GRAFSTEIN, B. 1956. Mechanism of spreading cortical depression. *J. Neurophysiol.* **19** 154–171.
- [5] GRAFSTEIN, B. 1963. Neuronal release of potassium during spreading depression. In: *Brain Function. Cortical Excitability and Steady Potentials*. M.A.B Brazier (Ed.), University of California Press, 87–124.
- [6] HADJIKHANE, N., DEL RIO, M.S., WU, O., SCHWARTZ, D., BAKKER, D., FISCHI, B., KWONG, K.K., CUTRER, F.M., ROSEN, B.R., TOOTELL, R.B.H., SORENSEN, A.G., AND MOSKOWITZ,

- M.A. 2001. Mechanisms of migraine aura revealed by functional MRI in human visual cortex. *Proc. Natl. Acad. Sci. (USA)* **98**, 4687–4692.
- [7] HINES, M. AND CARNEVALE, N.T. 1997. The NEURON simulation environment. *Neural Computat.* **9**, 1179–1209. URLs: <http://www.neuron.yale.edu/neuron/>, <http://neuron.duke.edu/>
- [8] HUANG, H., MIURA, R.M. AND YAO, W. 2010. A simplified neuronal model for the instigation and propagation of cortical spreading depression. Submitted.
- [9] KAGER, H., WADMAN, W.J., AND SOMJEN, G.G. 2000. Simulated seizures and spreading depression in a neuron model incorporating interstitial space and ion concentrations. *J. Neurophysiol.* **84** 495–512.
- [10] KAGER, H., WADMAN, W.J., AND SOMJEN, G.G. 2002. Conditions for the triggering of spreading depression studied with computer simulations. *J. Neurophysiol.* **88** 2700–2712.
- [11] KOCH, C. AND SEGEV, I. 1998. *Methods in Neuronal Modeling: From Ions to Networks.*, MIT Press, Cambridge, MA.
- [12] LÄUGER, P. 1991. *Electrogenic Ion Pumps*. Sinauer, Sunderland MA.
- [13] LEÃO, A.A.P. 1944. Spreading depression of activity in the cerebral cortex. *J. Neurophysiol.* **7**, 359–390.
- [14] NAGUMO, J., ARIMOTO, S., AND YOSHIZAWA, S. 1962. An active pulse transmission line simulating nerve axon. *Proc. IRE* **50**, 2061–2070.
- [15] SHAPIRO, B.E. 2000. An Electrophysiological Model of Gap-Junction Mediated Cortical Spreading Depression Including Osmotic Volume Changes. PhD Dissertation, Biomathematics, UCLA.
- [16] SHAPIRO, B.E. 2001. Osmotic forces and gap junctions in spreading depression: A computational model. *J. Comp. Neurosci.* **10**, 99–120.
- [17] SHIBATA, M. AND BUREŠ, J. 1975. Techniques for termination of reverberating spreading depression in rats. *J. Neurophysiol.* **38**, 158–166.
- [18] SOMJEN, G.G. 2004. *Ions in the Brain. Normal Function, Seizures, and Stroke*. Oxford University Press, Oxford, UK.
- [19] **Sugaya, E. Takato, M., and Y. Noda, Y. 1975. Neuronal and glial activity during spreading depression in cerebral cortex of cat. *J. Neurophysiol.* **38**, 822–841.**
- [20] TUCKWELL, H.C. AND MIURA, R.M. 1978. A mathematical model for spreading cortical depression. *Biophys. J.* **23**, 257–276.
- [21] WIENER, N. AND ROSENBLUETH, A. 1946. The mathematical formulation of the problem of conduction of impulses in a network of connected excitable elements, specifically in cardiac muscle. *Arch. Inst. Cardiol. Mex.* **16**, pp. 205–265.